

Extreme Rainfall and Flooding from Supercell Thunderstorms

JAMES A. SMITH, MARY LYNN BAECK, AND YU ZHANG

Department of Civil and Environmental Engineering, Princeton University, Princeton, New Jersey

CHARLES A. DOSWELL III

National Severe Storms Laboratory, Norman, Oklahoma

(Manuscript received 13 September 2000, in final form 25 May 2001)

ABSTRACT

Supercell thunderstorms, the storm systems responsible for most tornadoes, have often been dismissed as flood hazards. The role of supercell thunderstorms as flood agents is examined through analyses of storm systems that occurred in Texas (5–6 May 1995), Florida (26 March 1992), Nebraska (20–21 June 1996), and Pennsylvania (18–19 July 1996). Particular attention is given to the “Dallas Supercell,” which resulted in 16 deaths from flash flooding and more than \$1 billion in property damage during the evening of 5 May 1995. Rainfall analyses using Weather Surveillance Radar-1988 Doppler (WSR-88D) reflectivity observations and special mesonet rain gauge observations from Dallas, Texas, show that catastrophic flash flooding resulted from exceptional rainfall rates at 5–60-min timescales. The spatial structure of extreme rainfall was linked to supercell structure and motion. The “Orlando Supercell” produced extreme rainfall rates (greater than 300 mm h^{-1}) at 1–5-min timescales over a dense rain gauge network. The Nebraska and Pennsylvania storm systems produced record flooding over larger spatial scales than the Texas and Florida storms, by virtue of organization and motion of multiple storms over the same region. For both the Nebraska and Pennsylvania storms, extreme rainfall and tornadoes occurred in tandem. Severe rainfall measurement problems arise for supercell thunderstorms, both from conventional gauge networks and weather radar. It is hypothesized that supercell storms play a significant role in the “climatology” of extreme rainfall rates (100-yr return interval and greater) at short time intervals (1–60 min) in much of the central and eastern United States.

1. Introduction

During the past 20 years there have been major advances in understanding the dynamics of supercell thunderstorms and their role in tornadogenesis (see Doswell and Burgess 1993). Supercell storms have often been dismissed as heavy rainfall producers based on arguments revolving around low precipitation efficiency and rapid storm motion. Cotton and Anthes 1989, for example, note that “storms producing the largest hailstones occur in strongly sheared environments; thus, in general, we should not expect that the storm systems producing the largest hailstones are also heavy rain-producing storms.” Doswell et al. 1996 provide a different perspective, noting that “the combination of intense updrafts and substantial low-level moisture suggests some potential for heavy rainfall rates” (see also Moller et al. 1990, 1994; Doswell 1998).

The 559-mm rainfall accumulation during 2.75 h in D’Hannis, Texas, on 31 May 1935 is a world record

for the 2–3-h time period (WMO 1986). The *Hondo Anvil Herald* of 7 June 1935 noted that “a cyclone and severe electrical storm accompanied the rain” (see Dalrymple et al. 1937; “cyclone” is used colloquially to mean tornado), suggesting that a supercell thunderstorm contributed to this record. This observation is intriguing but raises more questions than it answers. How much rainfall was contributed in this case by supercell thunderstorms? Was there one storm or multiple storms? Were the storms moving rapidly or was anomalous storm motion a key ingredient of the rainfall record?

During the evening of 5 May 1995, a supercell thunderstorm (Fig. 1) passed over the Dallas–Fort Worth metropolitan area, producing softball-sized hail in Fort Worth and flash floods that resulted in 16 fatalities in Dallas. Total damages from flooding and hail made the “Dallas Supercell” the first \$1 billion thunderstorm in U.S. history (NOAA 1995). Unlike the 31 May 1935 storm, there were exceptional observations of the Dallas Supercell from the Dallas–Fort Worth Weather Surveillance Radar-1988 Doppler (WSR-88D) and a dense network of rain gauges in the Dallas metropolitan area.

In this paper, it is demonstrated that supercell thun-

Corresponding author address: James A. Smith, Environmental Engineering and Water Resources, Dept. of Civil and Environmental Engineering, Princeton University, Princeton, NJ 08544.
E-mail: jsmith@princeton.edu

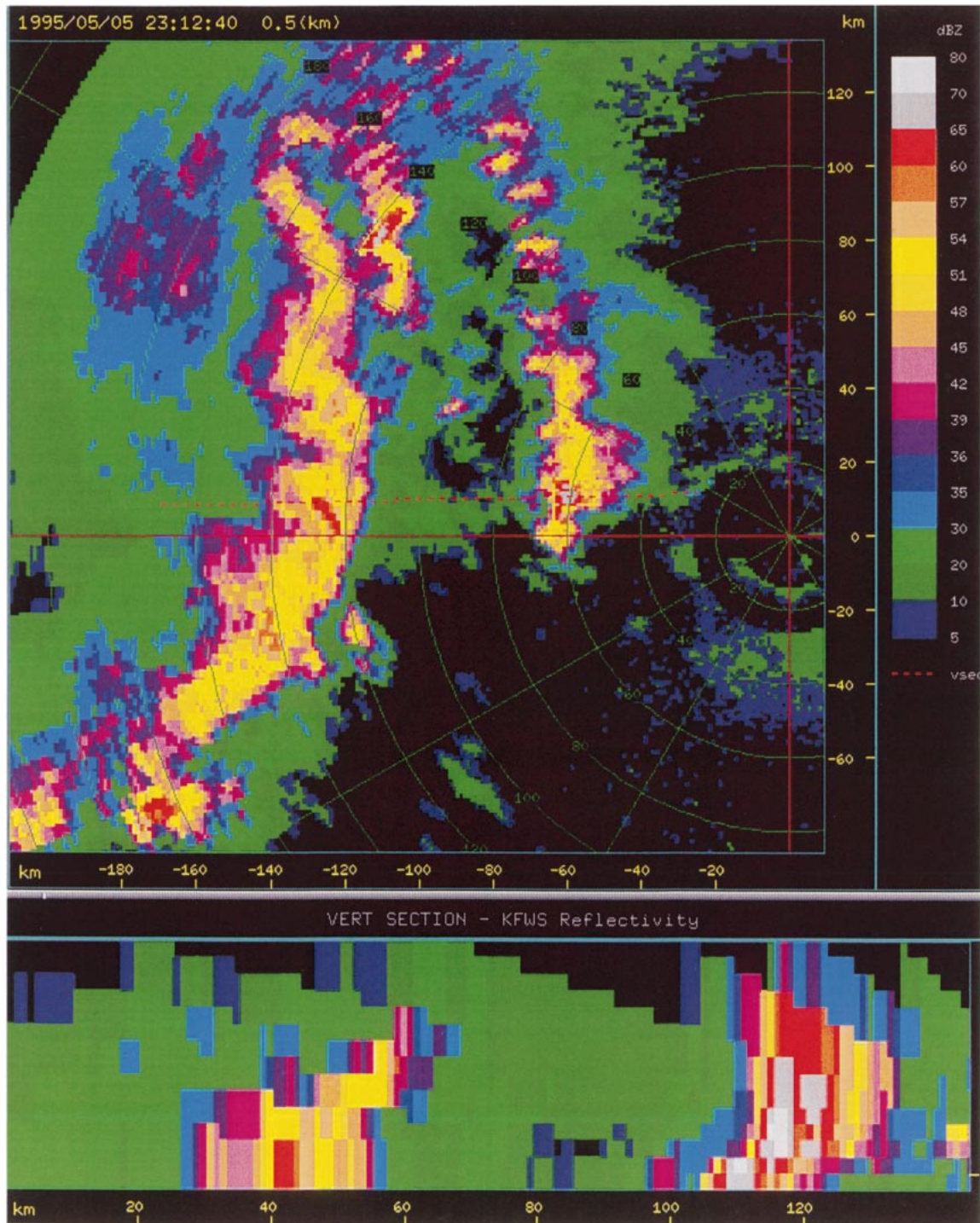


FIG. 1. Reflectivity image (0.5-km elevation) from the Dallas WSR-88D at 2312 UTC 5 May 1995 showing the Dallas Supercell approximately 30 km west of radar. Range rings are 20 km. Trailing squall line is approximately 50 km west of the Dallas Supercell. The bottom image depicts a vertical cross section along the dotted red line shown in the top image.

derstorms can indeed represent a major flood hazard by using analyses of the Dallas Supercell and three other storm systems that produced extreme rainfall and flooding in Florida (26 March 1992), Nebraska (21 June

1996), and Pennsylvania (18–19 July 1996). Locations and timing of the events are representative of the seasonal and geographic occurrence of supercell storms (as illustrated in the following sections). Detailed analyses

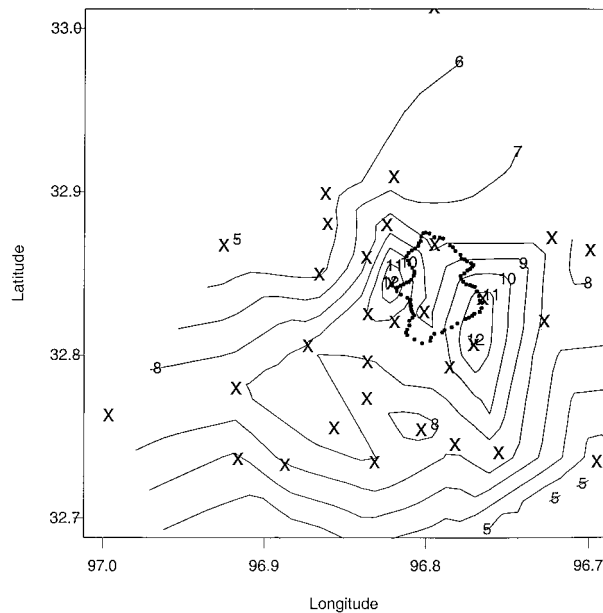


FIG. 2. Storm total rainfall distribution for 5–6 May 1995 over the Dallas metropolitan region, based on rain gauge observations from the Dallas mesonet (locations denoted by “x”). The boundary of Turtle Creek is outlined by dots. Contours represent storm total precipitation isohyets (cm).

of the Dallas Supercell are carried out, using the dense rain gauge observations along with WSR-88D radar observations to characterize spatial and temporal variability of supercell rainfall. The Orlando, Florida, storm provides a second opportunity to examine supercell rainfall over a dense rain gauge network. The Nebraska and Pennsylvania storm systems resulted in flooding at larger spatial scales than those of the Dallas Supercell and “Orlando Supercell,” owing to multiple storms tracking over the same area for an extended period of time. For both the Nebraska and Pennsylvania storms, extreme rainfall and tornadoes occurred in tandem over the flood area.

The objectives of this study are

- 1) to identify the aspects of supercell structure, motion, and evolution that control the spatial and temporal distribution of extreme rainfall and flooding;
- 2) to characterize the magnitude of rainfall rates and their relation to supercell structure and motion;
- 3) to provide a depiction of the “climatology” of extreme rainfall from supercell thunderstorms; and
- 4) to illustrate the rainfall measurement problem for supercell thunderstorms.

The focus of this paper is on the spatial and temporal structure of extreme rainfall from supercell thunderstorms. A particular motivation for this study is the desire to understand the scale-dependent hydrologic response of drainage basins for extreme flood events at basin scales ranging from 1 to 1000 km² (see Smith 1992; Gupta et al. 1994; Woods and Sivapalan 1999;

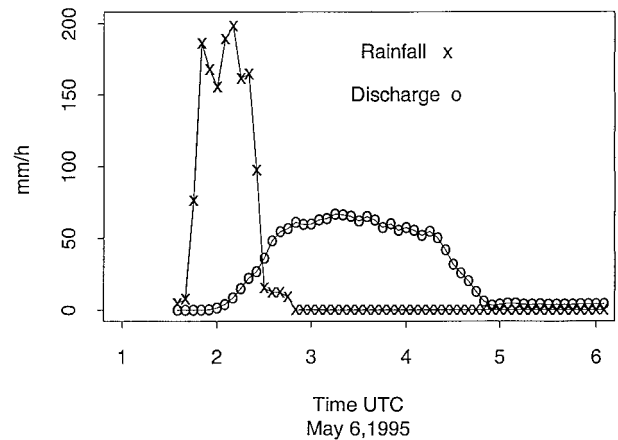


FIG. 3. Time series of basin-averaged rainfall (mm h^{-1} ; derived from rain gauge observations) and discharge (mm h^{-1}) for Turtle Creek (see Fig. 2 for basin boundary). Discharge is expressed as a unit discharge by dividing discharge ($\text{m}^3 \text{s}^{-1}$) by drainage area (km^2) and converting to millimeters per hour.

Smith et al. 2000). This study is further motivated by applications in engineering design that require detailed understanding of the geographic distribution of flood hazards associated with extreme rainfall. As noted in NRC (1994), there are particular difficulties in characterizing the spatial occurrence of extreme rainfall for short durations and small areas. This paper does not attempt to identify the physical mechanisms distinguishing supercell storms that produce extreme rainfall from those that do not (see, e.g., Moller et al. 1994). We do, however, attempt to identify physical mechanisms that control rainfall distribution at timescales and space scales relevant to flood production.

2. Dallas Supercell: 5–6 May 1995

The Dallas Supercell is illustrated in Fig. 1 through observations from the Dallas–Fort Worth WSR-88D. The supercell and squall line were moving eastward with speeds of approximately 40 and 60 km h^{-1} , respectively. Maximum reflectivity values in the supercell were 77 dBZ at the time of the volume scan shown in Fig. 1, and reflectivity values greater than 60 dBZ extended above 10 km. Reports of grapefruit-sized hail were received by the National Weather Service (NWS) at this time. The squall line overtook the supercell thunderstorm at approximately 0130 UTC along the western boundary of Dallas. Catastrophic rainfall during the 45-min period ending at 0215 UTC resulted in the 16 flash-flood deaths in Dallas. The synoptic-scale environment of the Dallas Supercell is summarized and discussed in the National Disaster Survey Report for the event (NOAA 1995).

The storm total rainfall distribution for the Dallas region (Fig. 2), as determined from the Dallas metropolitan rain gauge network, exhibited large spatial variability. Catastrophic rainfall and flooding were con-

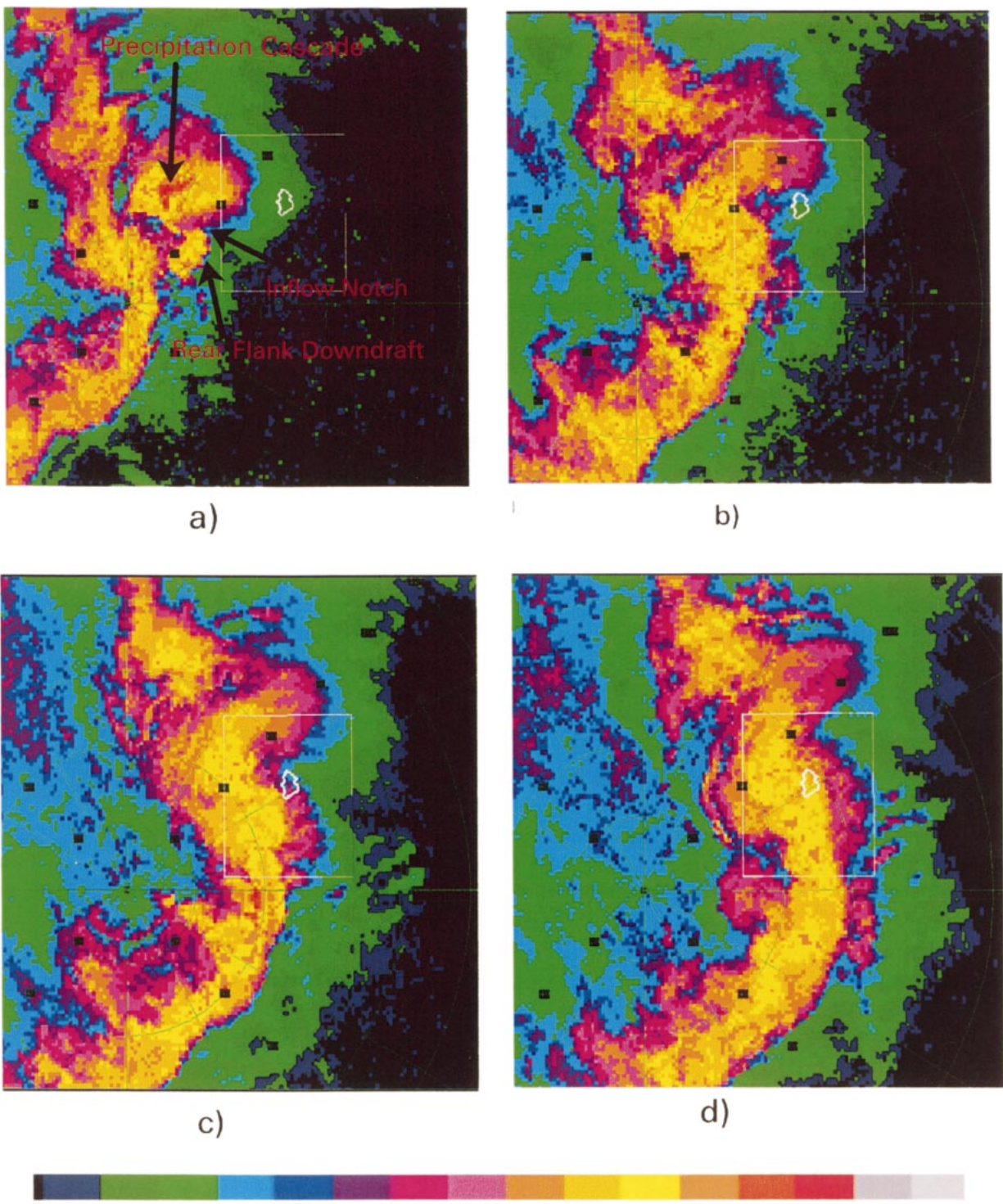


FIG. 4. Low-level (0.5 km) reflectivity images of Dallas Supercell and squall line at (a) 0057, (b) 0120, (c) 0132, (d) 0144, (e) 0201, and (f) 0219 UTC 6 May 1995. The white box corresponds to the region shown in Fig. 2. The basin boundary of Turtle Creek is outlined in white within the box.

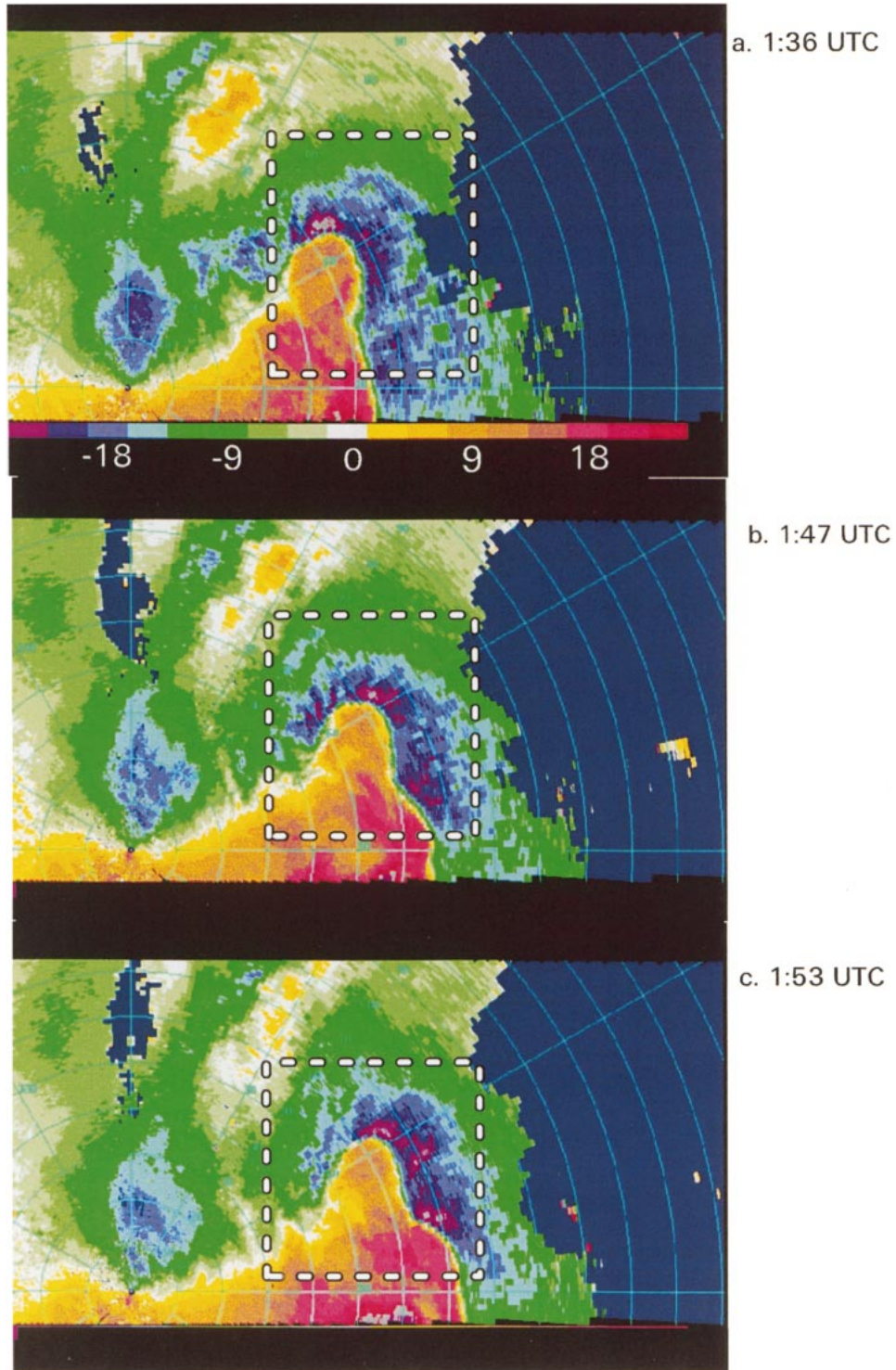


FIG. 5. Doppler velocity images from the 0.5° elevation angle at (a) 0136, (b) 0147, and (c) 0153 UTC. The white box corresponds to the region shown in Fig. 2 and the boxed region in Fig. 4.

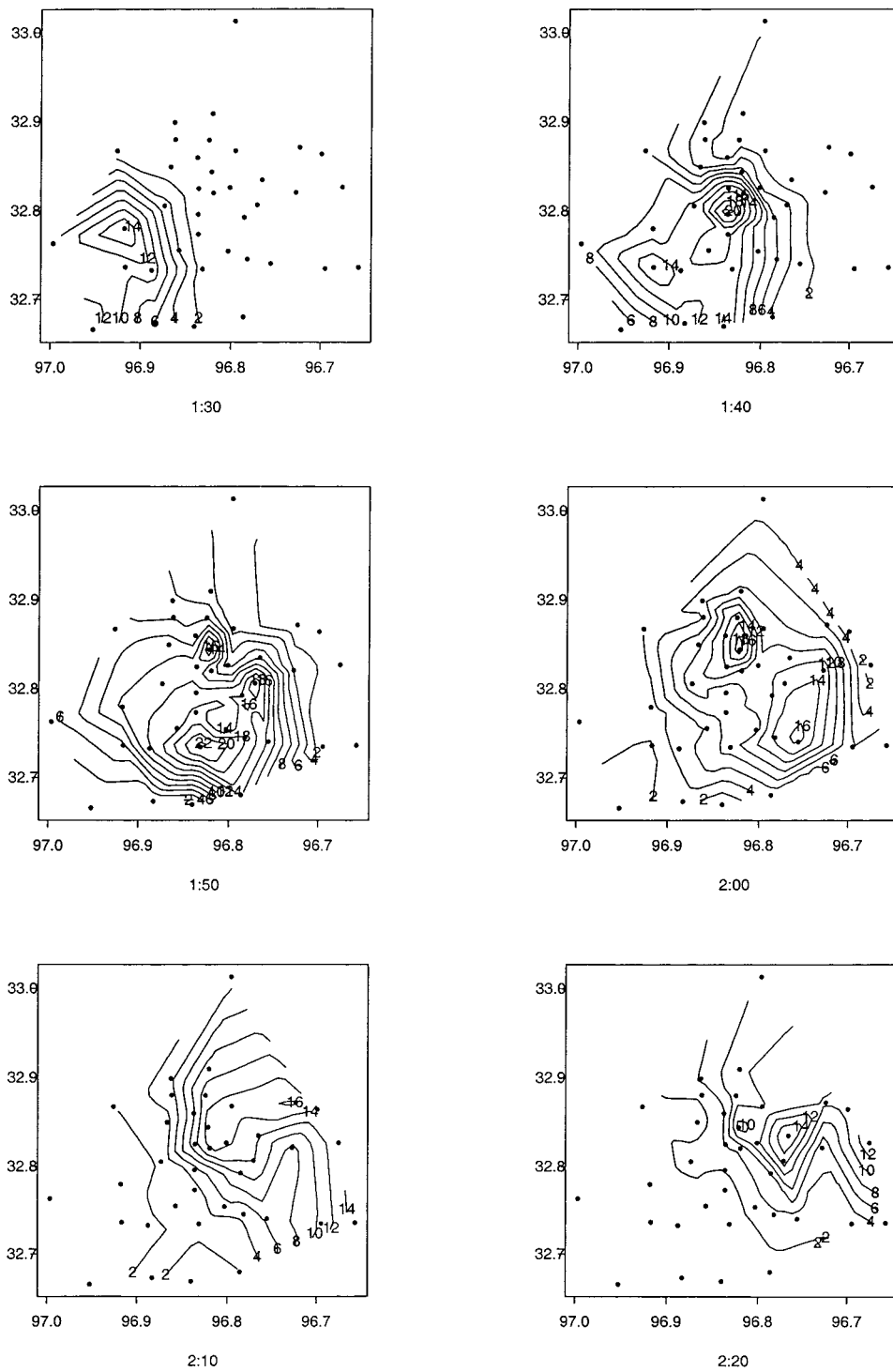


FIG. 6. Rainfall-rate (cm h^{-1}) contour maps for the Dallas metropolitan area during the period of 0125–0220 UTC 6 May (corresponding to the area in Fig. 2). Each contour map is derived from 5-min rainfall-rate observations at gauges (denoted by dots). The time period shown below each map is the ending time of the 5-min period for the rainfall field.

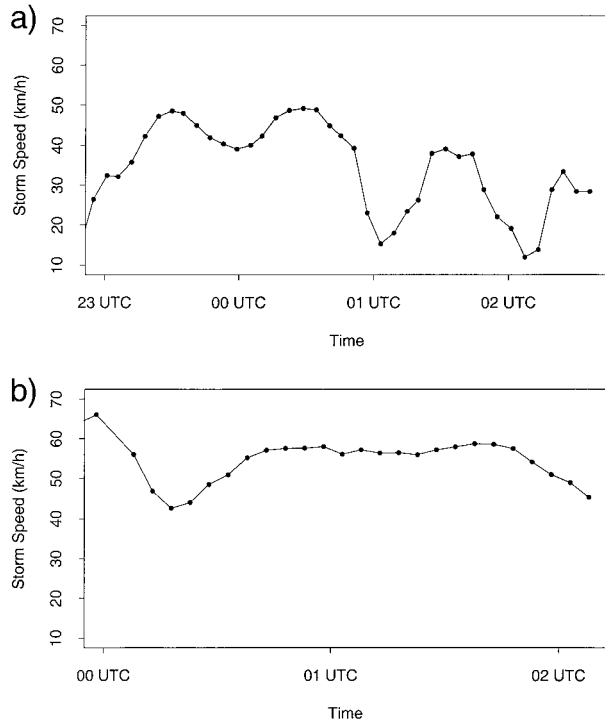


FIG. 7. Storm speed (km h^{-1}) for (a) the Dallas Supercell from 2300 UTC 5 May to 0230 UTC 6 May 1995 and (b) the Orlando Supercell from 0000 to 0200 UTC 26 Mar 1992.

centrated in a small area of central Dallas, with two maxima of 120 mm on the western boundary and south-eastern boundary of Turtle Creek. Spatial gradients of 50 mm over a distance of approximately 4 km separated the area of heaviest rainfall from the large swath of 50–70-mm storm total accumulations. The local maxima exceeding 120 mm on the western and southeastern boundary of Turtle Creek were associated with different structural elements of the Dallas Supercell, as detailed below.

Stream-gauging observations in Turtle Creek provided a 5-min record of water surface elevation. A discharge hydrograph (Fig. 3) was constructed from the stage observations using stage–discharge relations developed from observations reported in Band et al. (1982). The peak discharge at 20- km^2 drainage area was $400 \text{ m}^3 \text{ s}^{-1}$, resulting in a unit discharge, that is, discharge divided by drainage area, of $20 \text{ m}^3 \text{ s}^{-1} \text{ km}^{-2}$. The peak unit discharge can also be expressed as a runoff rate of 60 mm h^{-1} , which provides useful comparison with basin-averaged rainfall-rate time series (Fig. 3). The lag time (i.e., the time difference between time centroid of rainfall and peak discharge) for Turtle Creek at 20- km^2 scale was approximately 1.2 h. The lag time provides a useful timescale for analysis of space–time variability of rainfall over the catchment. For the 20- km^2 drainage basin of Turtle Creek, rainfall separated by more than 1.2 h will not contribute synchronously to the peak at the basin outlet. The lag time

for a drainage basin can be viewed as an upper bound on the timescales of rainfall distribution that are relevant to flood magnitudes at the basin outlet.

Volume-scan reflectivity and Doppler velocity fields (Figs. 4 and 5) for the period of 0130–0215 UTC illustrate storm-scale evolution during the period of heavy rainfall in Dallas. The links between storm structure and evolution and rainfall distribution can be inferred from 5-min rainfall fields derived from the Dallas mesonet rain gauge observations (Fig. 6). Combining the information from these analyses leads to the following conclusions.

- 1) Between 0130 and 0140 UTC, the key elements of storm structure (Figs. 5 and 4c) included an inflow *notch*, with inbound Doppler velocities greater than 25 m s^{-1} at the 0.5° elevation angle, a “precipitation cascade” centered at the apex of the inflow region and which drapes around the inflow region; a rear-flank downdraft (RFD) region, most clearly seen as the near-circular region of outbound Doppler velocities adjacent to the inflow notch and squall line; and the squall line, with a line of reflectivity values greater than 60 dBZ. The precipitation cascade is linked with the forward-flank downdraft of the supercell [see Lemon and Doswell (1979) and Weisman and Klemp (1986) for classical models of supercell thunderstorms]. At 0132 UTC (Fig. 4c) there is a region of lower reflectivity values at the southwestern boundary of Turtle Creek separating peak reflectivities in the precipitation cascade from those in the RFD.
- 2) Rainfall analyses for the 5-min period ending at 0150 UTC (Fig. 6) show a region of extreme rainfall rates to the rear of the RFD. A small region of increased rainfall rates is located to the northwest and is centered at approximately 32.85°N , 96.82°W . The largest 5-min rainfall rates for the event occurred in the RFD region along a 10-km southwest-to-northeast-oriented swath. Low-level inflow to the storm peaked between 0136 and 0147 UTC (Fig. 5 and additional images that are not shown).
- 3) At 0200 UTC, similar rainfall structure prevailed, with two key additional observations. The RFD region has moved, whereas the region of increased precipitation to the north has not (Figs. 4–6). Extreme rainfall rates for the northern region have expanded along the western margin of the Turtle Creek catchment.
- 4) From 0145 to 0220 UTC, the RFD moved at a speed of 30 km h^{-1} , the squall line (tracking the leading edge of the 0–Doppler velocity boundary) moved at 60 km h^{-1} , and the precipitation cascade remained virtually stationary. Motion of these three storm elements was closely related to the space–time distribution of flood-producing rainfall.

The composite motion of the supercell was computed from storm-tracking analyses of WSR-88D reflectivity

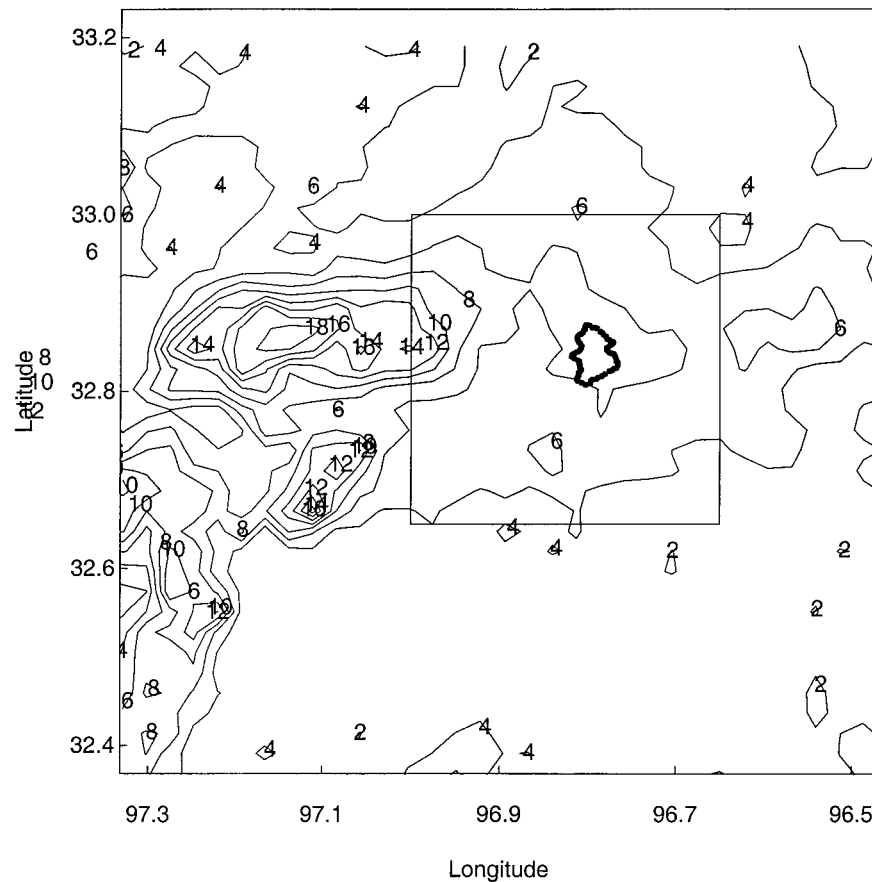


FIG. 8. Storm total rainfall (cm) field (2000 UTC 5 May–0400 UTC 6 May 1995) derived from volume-scan WSR-88D reflectivity observations using the WSR-88D $Z-R$ relationship ($Z = 300R^{1.4}$) and a 55-dBZ reflectivity threshold. The box corresponds to the region illustrated in Fig. 2, and the basin boundary of Turtle Creek is outlined as in Fig. 2.

observations. The motion vector is obtained from storm locations computed for each volume scan. Storm locations are the surface projection of the 3D center of mass of the storm (Dixon and Wiener 1993). The most important element of the analysis is that from 0130 to 0215 storm speed of the supercell decreased from 35 to less than 15 km h^{-1} (Fig. 7a). As noted above, storm speed from 0130 to 0215 UTC included differential rates of motion from the precipitation cascade and rear-flank downdraft. The net effect of storm speed was to increase rainfall accumulations dramatically at a 5–30-min time-scale.

The largest rainfall rates at 5-, 15-, and 60-min time intervals from the Dallas rain gauge network were, respectively, 231, 210, and 115 mm h^{-1} (no corrections have been made for systematic underestimation of rainfall rates, which for tipping bucket gauges can be significant at high rainfall rates; see Groisman and Legates 1994). The peak rainfall rates at 5-, 15-, and 60-min time intervals are respectively 87%, 110%, and 115% of the 100-yr rainfall rates for Dallas at these time intervals (265, 191, and 100 mm h^{-1} ; see Frederick et al. 1977). The peak 60-min rainfall effectively provides the

storm total rainfall for the event. Rainfall rates from the Dallas Supercell were most extreme at the 15–60-min time period, which is close to the lag time of the 20- km^2 Turtle Creek watershed. To place the rainfall magnitudes in a broader context, record rainfall observations for the conterminous United States range from 1860 mm h^{-1} at 1 min (Unionville, MD; 4 July 1956), to 437 mm h^{-1} at 42 min (Holt, MO; 22 June 1947) and 203 mm h^{-1} at 2.75 h (D'Hannis, TX; 31 May 1935).

Extreme rainfall rates can be obtained through various combinations of (a) large values of storm inflow velocity, humidity, and inflow area; (b) small values of surface rain area; (c) large rates of decrease in cloud water storage; and (d) small losses of water from the storm via evaporation. Surface observations on 5 May (not shown) show that wind speed increased steadily from 4 to 12 m s^{-1} during the 4-h period preceding storm arrival and that specific humidity increased from 8 g kg^{-1} at 1200 UTC to 16 g kg^{-1} immediately prior to storm arrival. Doppler velocity observations at 0136 UTC (Fig. 5) show a 10-km-wide region in the inflow notch of the storm with Doppler velocities that average 20 m s^{-1} (inflow is oriented in close to a radial direction

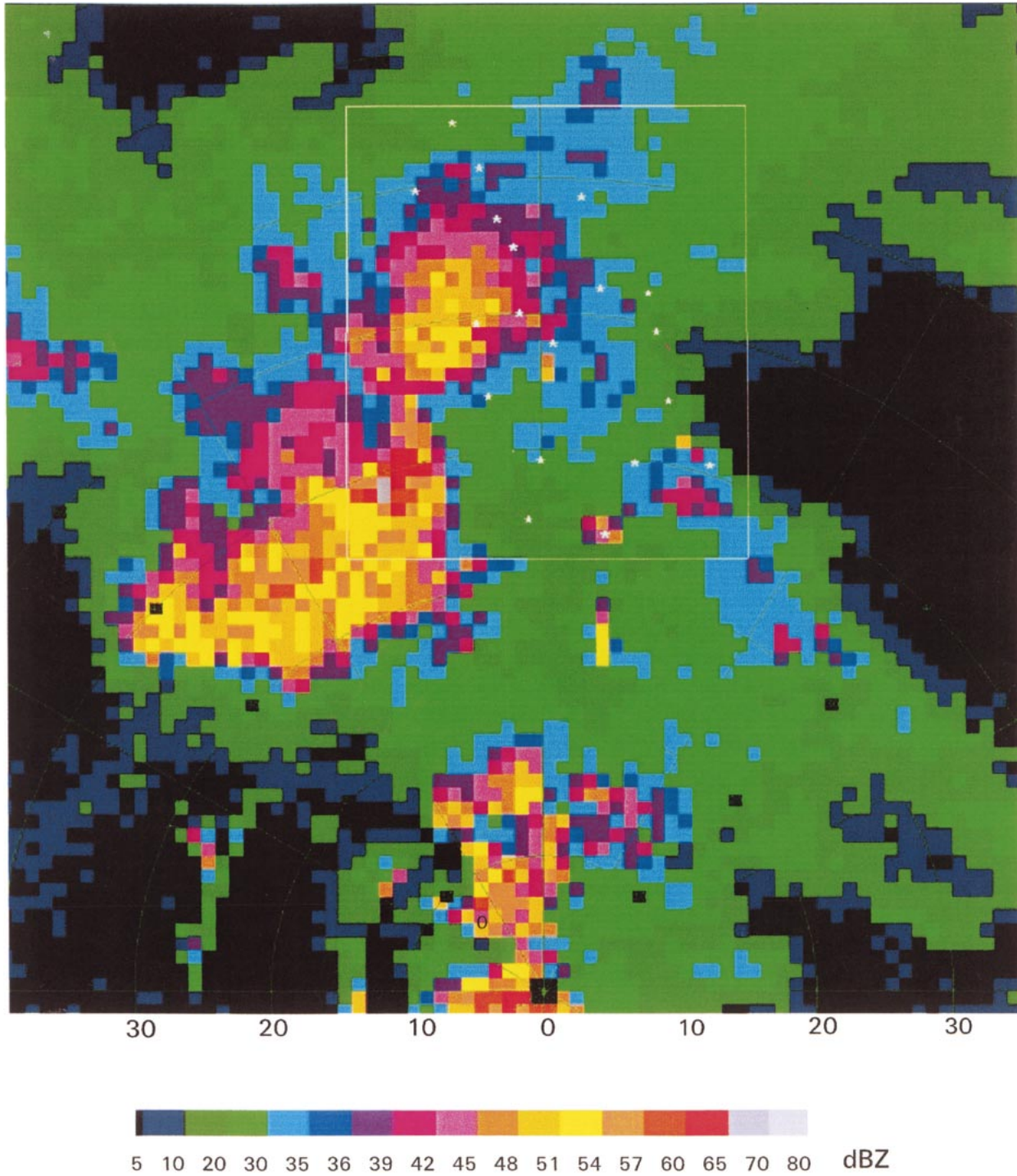


FIG. 9. Reflectivity image (0.5-km elevation) from the Melbourne, FL, WSR-88D at 0143 UTC 26 Mar 1992 illustrating the Orlando Supercell. Range rings are 10 km. The boxed region contains the KSC rain gauge network (Fig. 10), and dots indicate locations of rain gauges.

from the radar). If we take inflow width to be 10 km, inflow depth to be 2 km, inflow velocity to be 20 m s⁻¹, and specific humidity to be 12 g kg⁻¹, a cloud water balance would produce a rainfall rate of 104 mm h⁻¹

over 100 km², assuming an efficiency of 50% and no net change in cloud water storage. A doubling of the rainfall rate can be achieved by doubling the product of area, width, and inflow velocity or by decreasing the

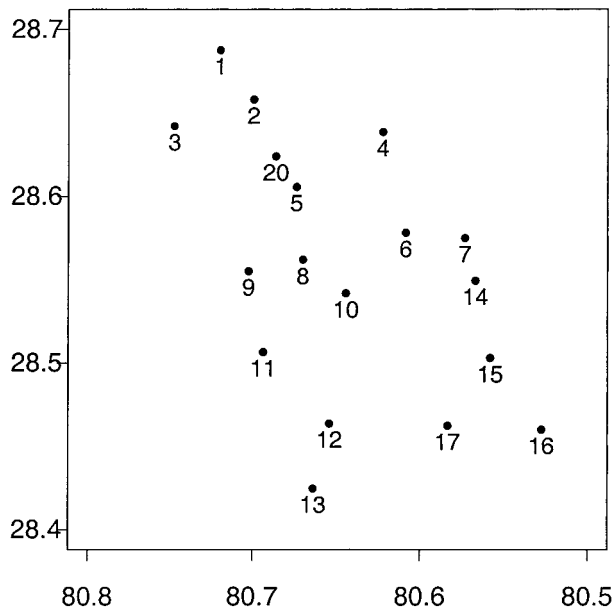


FIG. 10. Locations of rain gauges from the KSC network. Boxed region is the same as that shown in Fig. 9. Gauge numbers are used in time series plots of Fig. 12

area over which rainfall is distributed from 100 to 50 km². Precipitation efficiency clearly reflects only one aspect of the water budget representation of surface rainfall rates. Relatively low values of precipitation efficiency can be balanced by large values of moisture inflow (Doswell et al. 1996).

Interaction of the supercell with the overtaking squall line appears to have played an important role in the space-time rainfall distribution. Extreme rainfall rates in Dallas were associated with a *dissipating* supercell. Maximum reflectivity values decreased from 77 dBZ at 2300 UTC to 61 dBZ at 0200 UTC. Echo-centroid elevation decreased from 5.8 km above ground level at 2300 UTC to 3 km at 0200 UTC. The decreasing centroid elevation suggests that storage change may have played a role in the water budget of extreme rainfall rates for the Dallas Supercell.

As illustrated in Figs. 4 and 6, the spatial distribution of rainfall rate within the rain area plays an important role in determining maximum point rainfall rates. During the 5-min period of peak rainfall rates ending at 0150 UTC (Fig. 6), rainfall rates that exceeded 50 mm h⁻¹ covered a region of 427 km². The mean rainfall rate over this region was 113 mm h⁻¹. The subareas with rainfall rate that exceeded 100, 150, and 200 mm h⁻¹ were, respectively, 242, 89, and 7 km².

One of the major obstacles to a better understanding of the role of supercell storms as flood hazards is the difficulty of measuring rainfall for these storms. Neither conventional weather radar observations nor observations from operational rain gauge networks provide a reliable observational basis for analyzing supercell rain-

fall. Analysis based on the standard WSR-88D Next-generation Weather Radar $Z-R$ relationship ($Z = 300R^{1.4}$, where Z is radar reflectivity and R is rainfall rate), with a 55-dBZ reflectivity cap and Dallas WSR-88D reflectivity observations shows peak storm total rainfall over Fort Worth instead of Dallas [Fig. 8; see Baeck and Smith (1998) for algorithm details and discussion of difficulties in measuring extreme rainfall rates from radar reflectivity observations). The analysis captures the west-to-east movement of the supercell but does not capture the peak rainfall in Dallas. Reflectivity-based methods for estimating rainfall from radar will often be compromised by hail contamination. The problem with hail contamination can be seen by observing that a 10-mm hydrometeor in a 1-m³ sample volume has the same reflectivity, 10⁶ mm⁶ m⁻³ (or 60 dBZ), as 10⁶ hydrometeors of 1-mm diameter in the same volume. The presence of hail in a radar sample volume can seriously degrade the capability of resolving extreme rainfall rates by radar. Use of the 55-dBZ cap presumes that the sample volume contains a mixture of hail and heavy rainfall. Radar polarimetric measurements (see Zrnić and Ryzhkov 1999) provide significant potential for eliminating hail-contamination problems in estimating rainfall from weather radar.

Operational rain gauge networks are also unable to capture the rainfall distribution from supercell thunderstorms. Rain gauge spacing from conventional networks is inadequate to resolve spatial patterns of rainfall associated with storm structure (as illustrated in Figs. 4–6). Rain gauges from the operational network in the Dallas metropolitan area sampled the periphery of the storm and consequently did not capture the maximum rainfall over Dallas.

3. Orlando Supercell: 26 March 1992

The Orlando Supercell of 26 March 1992 (Fig. 9) passed over Orlando, Florida, producing severe hail damage, and then passed over the Kennedy Space Center (KSC) mesonet (Fig. 10). For the 26 March 1992 storm, 18 of 20 rain gauges were operational and provided rainfall-rate observations at 1-min time interval. The largest 1-min rainfall rate measured at the KSC mesonet during the period of 1988–93 of 330 mm h⁻¹ occurred when the Orlando Supercell passed over the network. In this section, structure, motion, and rainfall of the Orlando Supercell are compared with those of the Dallas Supercell.

There were a series of large hail reports associated with the Orlando Supercell from 0000 to 0100 UTC 26 March 1992. The largest report was for a 3-in.-diameter hailstone at approximately 0045 UTC. Maximum reflectivity values for the storm decreased from 76 dBZ shortly before 0000 UTC to 60 dBZ at 0200 UTC. By 0132 UTC (Fig. 11), the RFD region of the supercell had begun to surge ahead of the storm center, beginning the transition from supercell to bow echo (Moller et al.

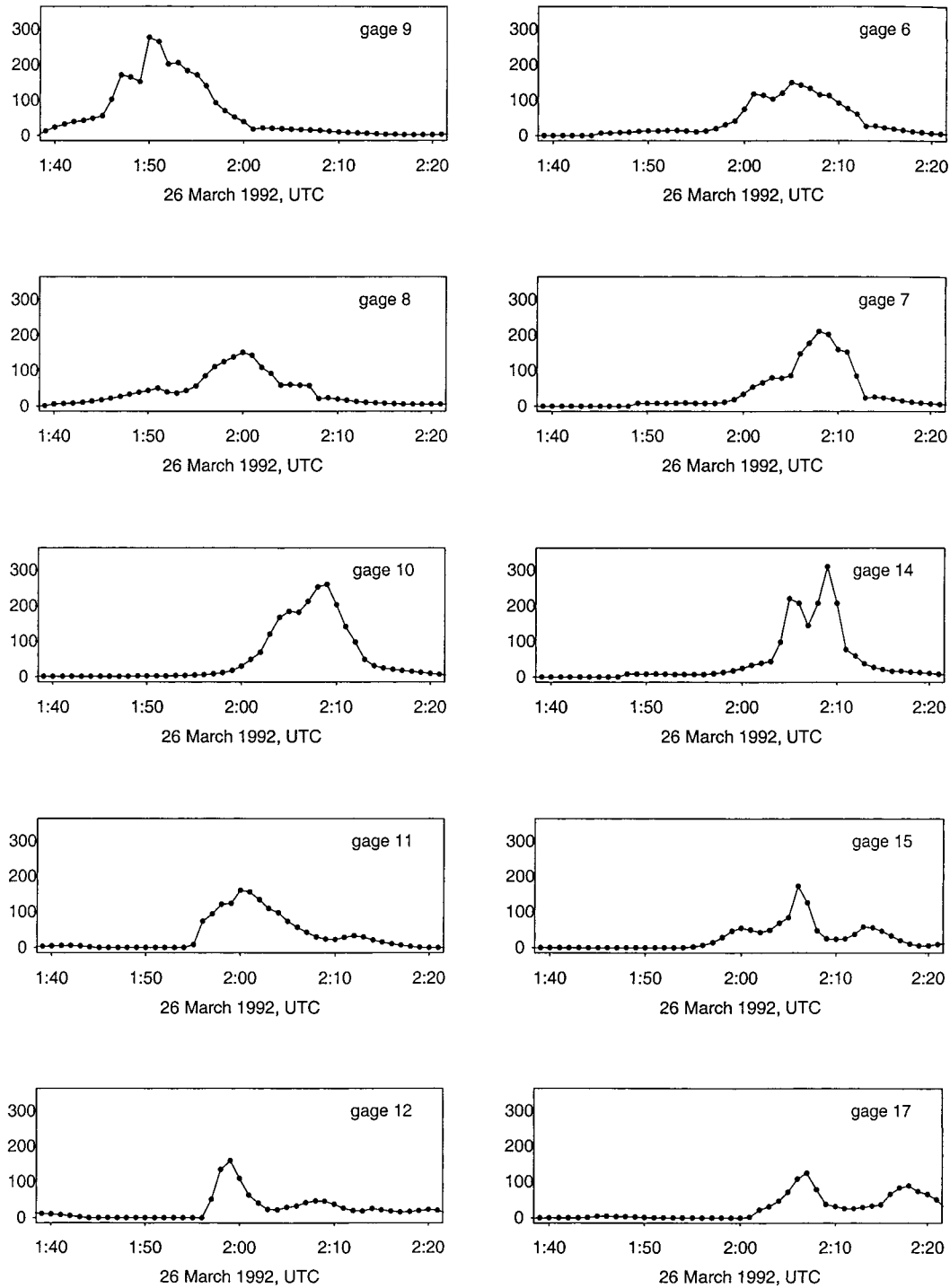


FIG. 12. Time series of 1-min rainfall rate (mm h^{-1}) for 10 rain gauges from the KSC network. Gauge numbers given in the upper-right-hand corner of each time series plot correspond to the identification numbers in Fig. 10.

1994; Przyblinski 1995). Storm structure of the Orlando Supercell at 0145 UTC (Fig. 9), immediately preceding the time when extreme rainfall was observed at the KSC mesonet, included a precipitation cascade and an RFD region. The KSC mesonet sampled rainfall from the

precipitation cascade with only the southernmost gauges sampling rainfall from the expanding RFD region.

Rain gauge observations from the KSC network (Fig. 12) illustrate the role of storm motion for space-time rainfall variability. A major control of space-time rain-

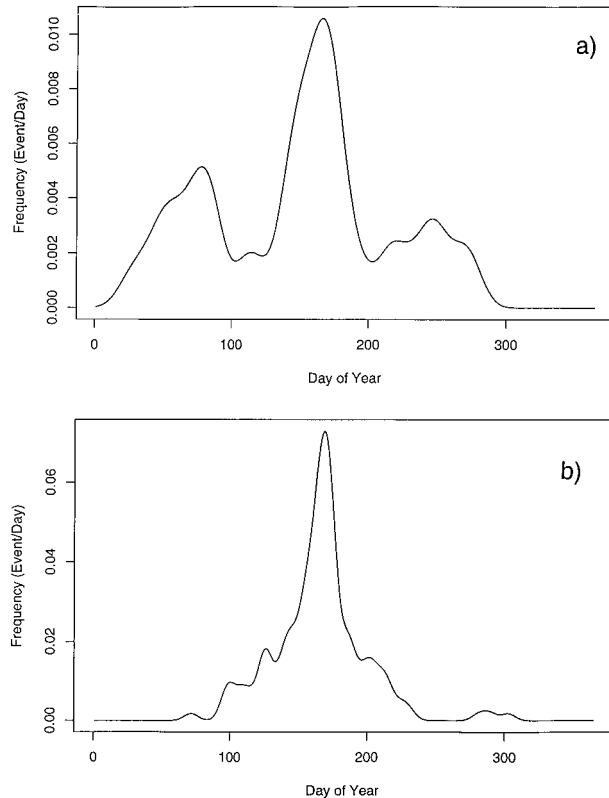


FIG. 13. (a) Seasonal frequency (events per day) of flood peaks in Maple Creek. (b) Seasonal frequency (events per day) of tornadoes for counties drained by Maple Creek.

fall variability is the west-to-east motion of the precipitation-cascade region through the center of the KSC network. The west-to-east progression of the heavy-rain region from 0150 to 0210 is clearly seen in the time series of rainfall progressing from gauge 9 to gauge 8 to gauge 10 (Fig. 12). Interpretation of space-time rainfall variability as resulting from a steady-state storm of fixed size moving at uniform speed is, however, not consistent with analyses in Fig. 12. Most notable, from 0205 until 0215 the eastern gauges 7 and 14 peak synchronously with the central gauge 10 at rain rates larger than 200 mm h^{-1} . Superimposed on variability associated with mean storm motion is large temporal variability associated with storm evolution and spatial variability associated with storm microstructure.

Rainfall rates for the Orlando Supercell were most exceptional at the shortest timescales (1–5 min). Peak rainfall rates ranged from 330 mm h^{-1} at 1 min to 222 mm h^{-1} at 5 min, 136 mm h^{-1} at 15 min and 37 mm h^{-1} at 60 min. The maximum rainfall rate at 5-min time interval (222 mm h^{-1}) was 85% of the 100-yr, 5-min rainfall rate for the region (Frederick et al. 1977; precipitation frequency estimates are not provided at timescales of less than 5 min). At 15-min timescales, the maximum rainfall rate (136 mm h^{-1}) was 70% of the 100-yr rainfall rate for the east coast of Florida. The

maximum hourly rainfall rate was not exceptional for Florida.

Storm speed for the Orlando Supercell is contrasted in Fig. 7b with that of the Dallas Supercell (Fig. 7a). Storm speed remained nearly constant at approximately 55 km h^{-1} , unlike the Dallas Supercell, for which storm speed slowed dramatically following merger with the trailing squall line. Because of steady, rapid storm motion, extreme rainfall rates over the KSC rain gauge network were limited to very short time intervals (1–5 min) and storm total accumulations were modest (less than 50 mm).

4. Nebraska: 20–21 June 1996

A series of tornadic supercell thunderstorms tracked through eastern Nebraska on 20–21 June 1996, producing record flooding at a number of U.S. Geological Survey (USGS) stream-gauging stations. In this and the following section, attention shifts from storm systems that produce extreme floods at small basin scales ($<20 \text{ km}^2$) to those that produce extreme floods at larger spatial scale ($>100 \text{ km}^2$). Analyses presented in this section are based largely on WSR-88D observations and stream-gauging observations. The focus of these analyses is the Pebble Creek watershed, for which virtually all rainfall was associated with supercell thunderstorms. Pebble Creek, located in eastern Nebraska, has a drainage area of 528 km^2 . It is bounded on the west by Maple Creek, a 1165-km^2 catchment with a stream-gauging record of more than 40 yr.

The long-term observed frequency of flooding in eastern Nebraska is characterized by a sharp peak in seasonal flood frequency (Fig. 13a, based on Maple Creek annual flood peak observations) during late June. June storms in eastern Nebraska are prominently represented in the occurrence of catastrophic rainfall in small areas of the United States. Three of 25 storms with measured rainfall exceeding 50% of probable maximum precipitation for the United States east of the Rocky Mountains (6-h duration, 10-mi^2 area) occurred in and near Maple and Pebble Creeks (Riedel and Schreiner 1980; Foufoula-Georgiou and Wilson 1990).

The seasonal occurrence of tornadoes (Fig. 13b) for the counties in and adjacent to Maple and Pebble Creeks exhibits a sharp late-June peak, corresponding in time with the peak in flood occurrence. The joint occurrence of flood events in Maple Creek (based on the partial-duration flood record series) and tornadic thunderstorms was examined by determining the flood events in Maple Creek for which a tornado report occurred the previous day (based on tornado reports for counties which Maple Creek drains). During the 1990s, there were seven flood events that could be linked in this manner to tornadoes. The count drops to three in the 1980s, one during the 1970s, four during the 1960s, and none in the 1950s. The increase in incidence of floods that are linked to tornadoes over time is probably related to increased de-

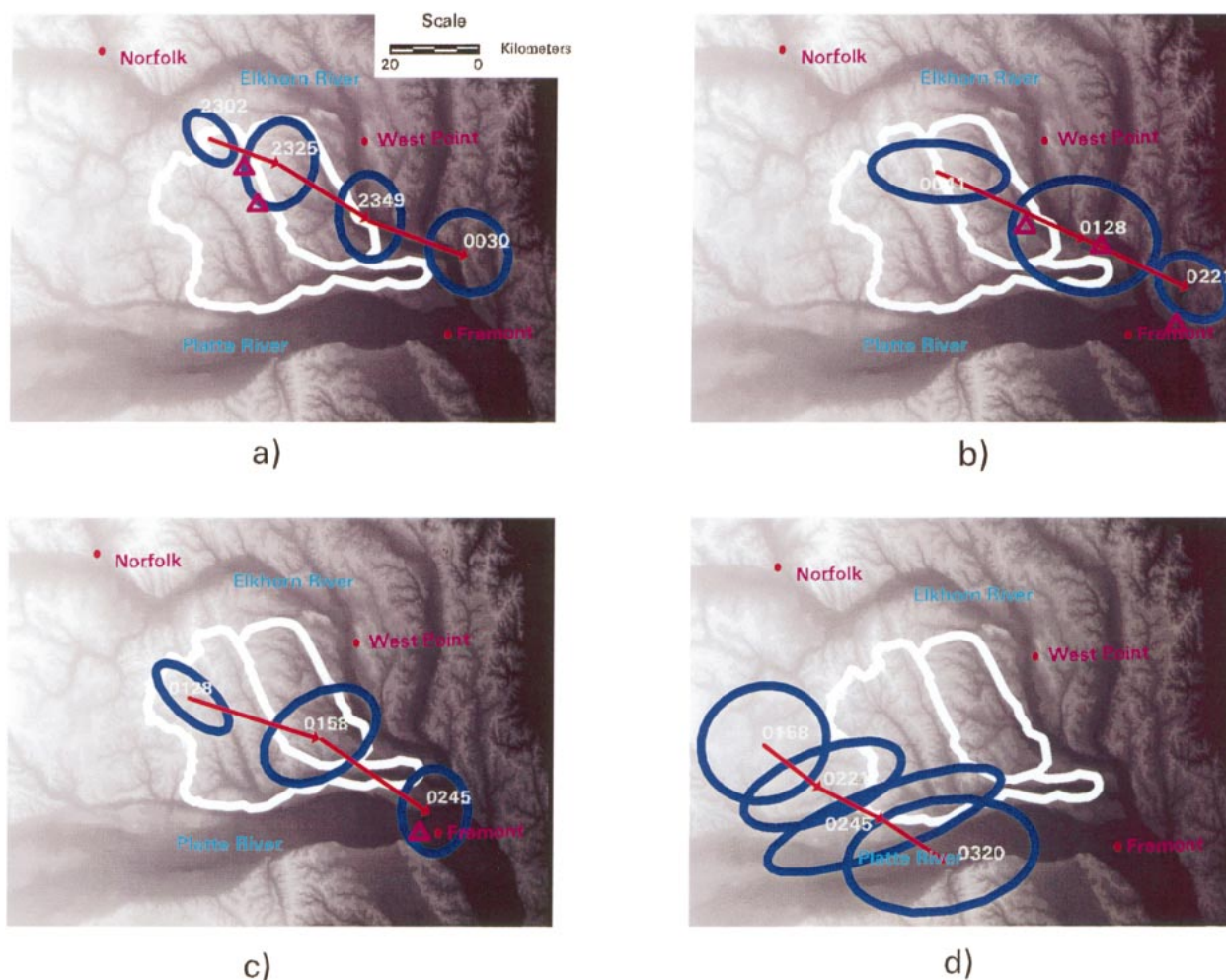


FIG. 14. Structure and motion of four supercell thunderstorms that passed over Maple and Pebble Creeks from 2300 UTC 20 Jun to 0300 UTC 21 Jun 1996. Ellipses contain the 45-dBZ boundary of the storm (in three dimensions). Volume-scan times are shown for each ellipse. Red triangles denote locations of tornado reports. The Pebble Creek basin boundary is outlined in white and is bordered on the southwest by the Maple Creek boundary (see Fig. 13a). The Platte and Elkhorn Rivers are labeled, along with the towns of Norfolk, West Point, and Fremont, NE.

tection of tornadoes with time. Even with these detection problems, it is clear that tornadic thunderstorms are a significant contributor to the flood behavior of the region. Six of the largest 14 flood peaks in the 40-yr Maple Creek record are linked to tornadic storm systems. Included are large floods during major tornado outbreaks on 14 June 1967, 17 June 1984, and 4 June 1992.

Extreme flooding in Pebble Creek on 21 June 1996 resulted from a series of four supercell storms that passed over the basin during a 4-h period from 2300 UTC June 20 to 0300 UTC June 21 (Fig. 14). For each of the storms and for the time periods shown in Fig. 14, storm motion was rapid and toward the southeast. Average storm speed during the periods shown in Fig. 14 was approximately 60 km h^{-1} . Each of the storms produced one or more tornadoes (Fig. 14) as they passed over Pebble Creek and Maple Creek. The storm systems that produced extreme rainfall in Dallas and Orlando

were dissipating supercells, in contrast to the Nebraska storms, which produced six tornadoes in and adjacent to Pebble Creek.

Structure and motion of the four storms illustrated in Fig. 14 played a prominent role in determining space-time variability of rainfall viewed from the Eulerian perspective imposed by the Pebble Creek drainage basin (Figs. 15–16). Rainfall analyses are based on WSR-88D volume-scan reflectivity observations and are computed using the standard WSR-88D Z - R relationship $Z = 300R^{1.4}$ with a 55-dBZ hail threshold. The fractional coverage of heavy rainfall (Fig. 16) is the fractional basin area with rainfall rates that exceed 25 mm h^{-1} . The normalized distance (Fig. 16; see Smith et al. 2001, manuscript submitted to *J. Hydrometeor.*) is the rainfall-rate-weighted distance to the basin outlet (with distance measured along the drainage network) divided by the maximum distance to the outlet. Values close to 0 in-

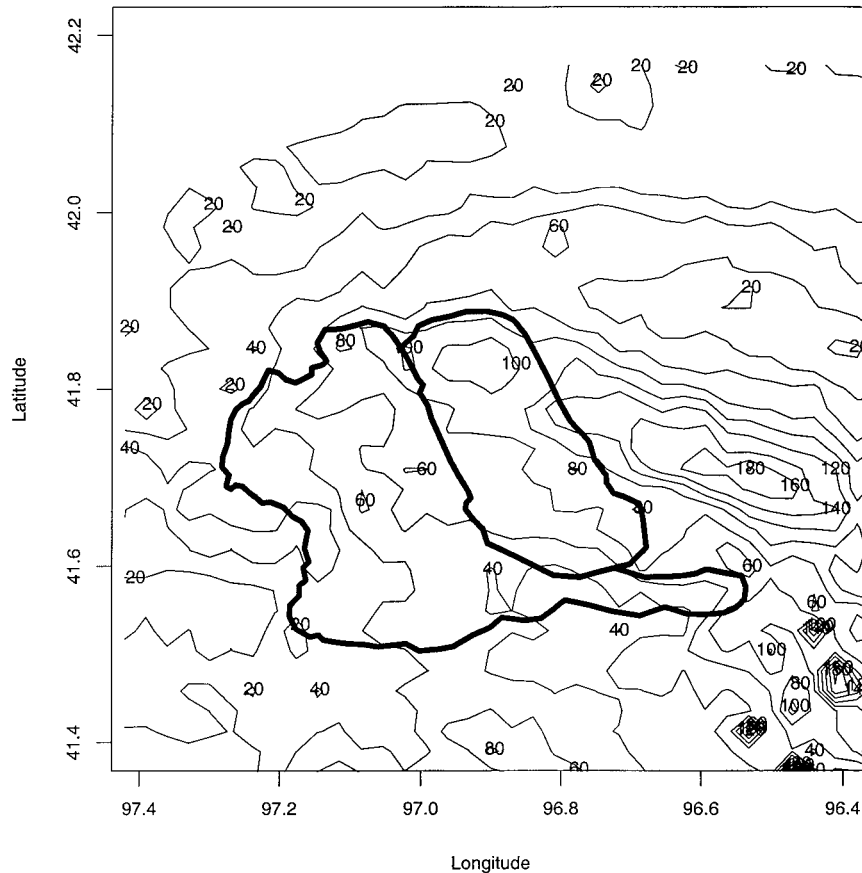


FIG. 15. Storm total rainfall (cm) field (2000 UTC 20 Jun–0600 UTC 21 Jun 1996) derived from volume-scan WSR-88D reflectivity observations using the WSR-88D $Z-R$ relationship ($Z = 300R^{1.4}$) and a 55-dBZ reflectivity threshold. Basin boundaries for Pebble Creek and Maple Creek are shown.

dicating a spatial rainfall distribution concentrated at the outlet of the basin; values close to 1 indicate that rainfall is concentrated at the periphery of the basin. Spatially uniform rainfall (solid line in Fig. 16) results in a value of 0.56 for the normalized distance.

The storm total rainfall distribution (Fig. 15) reflects southeast motion of the four storm elements and the southwestward shift of the tracks of the storms (Fig. 14). Basin-averaged rainfall for Pebble Creek was 85 mm. The rainfall accumulations estimated by radar are large, but not as exceptional as implied by the measured runoff. The basin-averaged runoff of 43 mm resulted in a runoff ratio (i.e., runoff divided by rainfall) greater than 50%. The average runoff ratio for the summer season in Pebble Creek is less than 10%. The 43 mm of runoff is 40% of the average annual runoff for Pebble Creek. Given the difficulties in measuring supercell rainfall by radar described in section 2, it is possible that the rainfall estimates are low.

A key element of the 20–21 June storms for flood production in Pebble Creek was the organization of heavy rainfall into a 4-h time period. The lag time of 10.3 h for the Pebble Creek flood peak was approxi-

mately 2.5 times the duration of extreme rainfall (4 h). Similar timing characterized the Turtle Creek flooding in Dallas at 20-km² scale with a lag time of 1.2 h and heavy rainfall duration of approximately 30 min. The temporal maximum in rainfall distribution occurred at approximately 2330 UTC on 20 June and was associated with storm 1 (Fig. 14). Fractional coverage of heavy rainfall reached a maximum of 50% (more than 250 km²) at 0120 UTC as storm 2 passed through the watershed (compare with spatial analyses of extreme rain area for the Dallas Supercell from dense rain gauges in section 2). The southeasterly motion of the storm elements resulted in downbasin storm motion, as reflected in decreasing values of the normalized distance (Fig. 16) during the two periods of heaviest rainfall: 2300–0000 UTC and 0030 UTC–0230 UTC. Storm size, motion at 528-km² and net duration all contributed to the peak discharge in Pebble Creek scale.

5. Pennsylvania: 18–19 July 1996

The western margin of the central Appalachian region rivals the Edwards Plateau of Texas (as typified by the

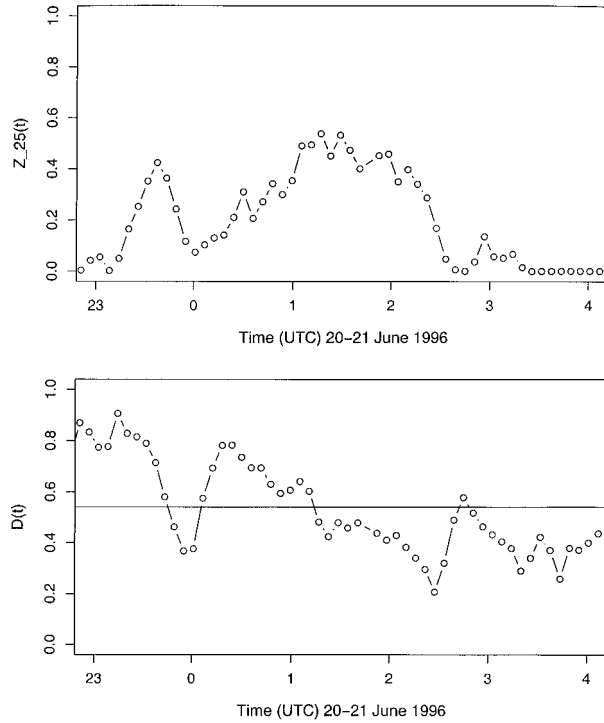


FIG. 16. Time series of (top) fractional coverage of heavy rainfall [$Z_{25}(t)$; fraction of basin area with rain rate $>25 \text{ mm h}^{-1}$] and (bottom) normalized distance function (see text). The solid line denotes the normalized distance for spatially uniform rainfall.

May 1935 D'Hannis storm noted in the introduction; see Costa 1987) for observations of extreme rainfall. The 483-mm rainfall accumulation in 2 h and 10 min on 18 July 1889 at Rockport, West Virginia (Finley 1889; Jennings 1950), was produced by a "terrific thunderstorm, accompanied by torrents of rainfall and vivid lightning" (Finley 1889). The world record rainfall accumulation of 782 mm in 4 h was produced by a thunderstorm complex in western Pennsylvania during the night and morning of 18–19 July 1942. Frequent lightning and hail accompanied the storms (Eisenlohr 1952). Extreme flooding occurred in the Redbank Creek watershed of western Pennsylvania on 18–19 July 1996 in connection with a major tornado outbreak in Pennsylvania (Pearce et al. 1998). The date of occurrence of the 1889, 1942, and 1996 flood events, 18–19 July is not purely fortuitous. There is a sharp seasonal maximum in heavy rainfall occurrence around 18 July (Fig. 17) that coincides with the peak in tornado occurrence for the region (not shown). Other major summer-season flood episodes in the western margin of the central Appalachians are described in Showalter (1941), Erskine (1951), NOAA (1991), and Bosart and Sanders (1981). The July 1996 Redbank Creek storm and flooding are examined in this section as a prototype for summer-season storms that produce catastrophic rainfall along the western margin of the central Appalachians and to

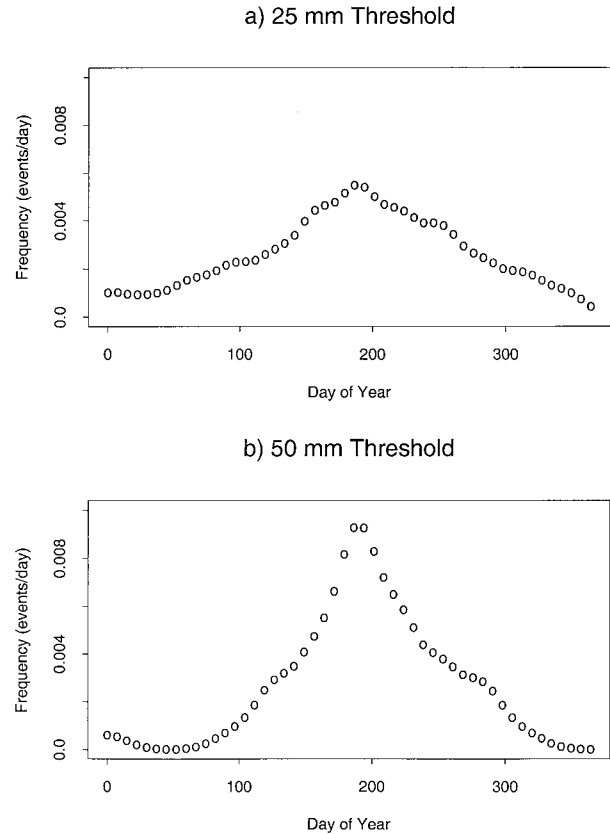


FIG. 17. Rate of occurrence of rainfall accumulations (24 h) exceeding (a) 25 and (b) 50 mm for the Franklin rain gauge in western PA.

illustrate the role of supercell storms in central Appalachian flood occurrence.

The 18–19 July 1996 storm produced the flood of record in Redbank Creek at a drainage area of 1368 km^2 from a stream-gauging record of more than 70 yr. The July 1996 flood peak of $1877 \text{ m}^3 \text{ s}^{-1}$ was 33% larger than the previous record peak. The second- and third-largest flood peaks resulted from the rain and snowmelt event of March 1936 and Hurricane Agnes in June of 1972 (note the striking connection to the three-floods paradigm of Miller 1990). The heaviest rainfall from the 1942 Smethport storm fell in upstream reaches of the Allegheny River (Redbank Creek is a tributary to the Allegheny River below the area of heaviest rainfall in 1942). The peak discharge of the Allegheny River at Eldred (1425 km^2) in July of 1942 was slightly smaller than the peak discharge from Redbank Creek in July of 1996. Peak discharge estimates for the July 1942 event (which are based on an extensive set of slope–area peak measurements conducted by the USGS) were most exceptional at the $1\text{--}100\text{-km}^2$ scale (Eisenlohr 1952, Costa 1987). Unlike the July 1942 storm (Eisenlohr 1952), there is no record of peak discharges at small basin areas within Redbank Creek for the July 1996 storm.

Extreme flooding in Redbank Creek resulted from a

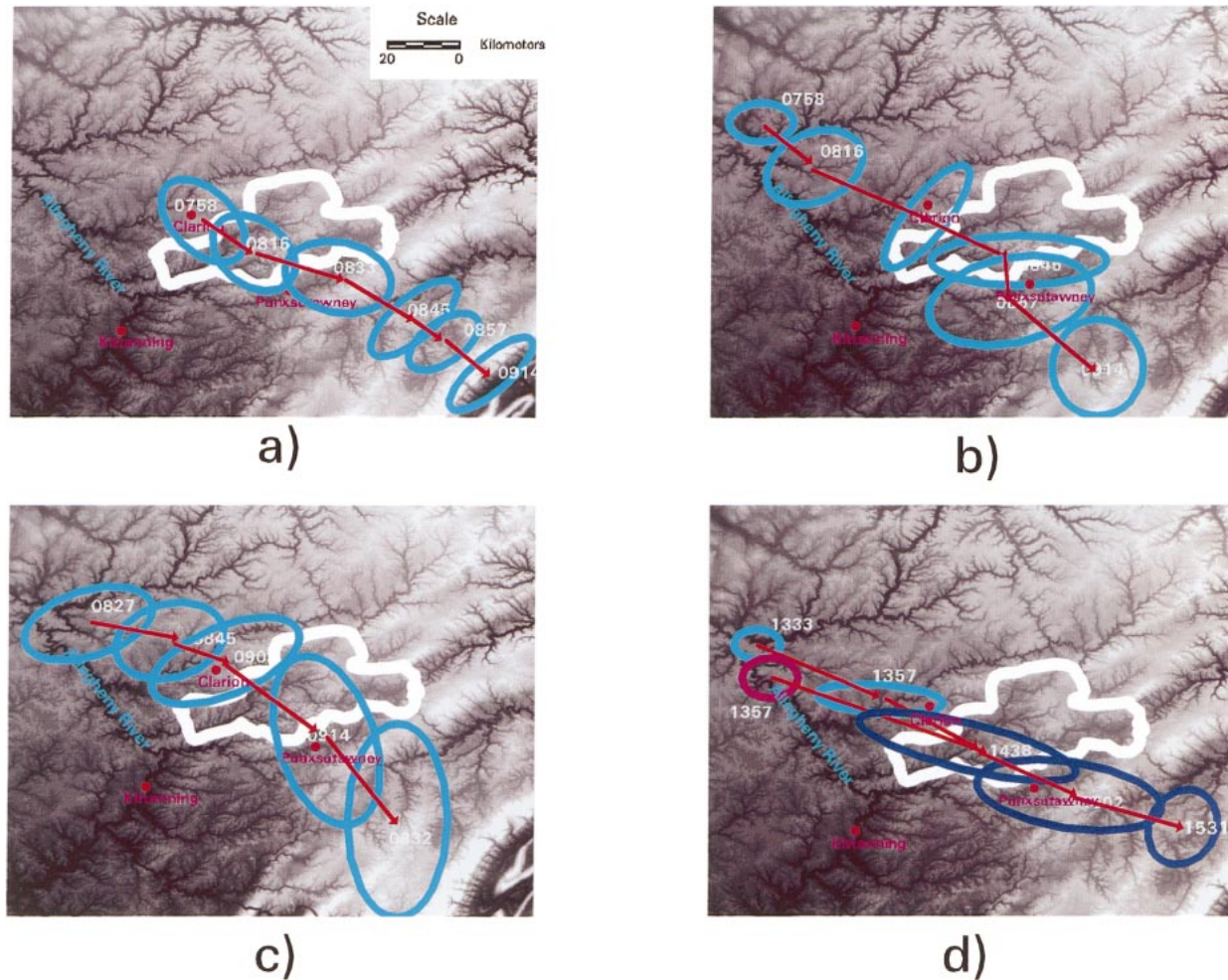


FIG. 18. Structure and motion of four storms that passed over Redbank Creek from 0600 to 1500 UTC 19 Jul 1996. Ellipses contain 45-dBZ boundary of the storm (in three dimensions). Volume-scan times are shown for each ellipse. The Redbank Creek basin boundary is outlined in white. The Allegheny River is labeled, along with the towns of Kittanning, Clarion, and Punxsutawney, PA. The storm ellipse for 1438 in (d) results from the merger of the two 1357 storm elements.

series of storms that passed over the basin from 0600 to 1500 UTC on 19 July 1996. Structure and motion of four storm elements are illustrated (Fig. 18) through a series of storm locations and storm area. Storms 1–3 (Figs. 18a–c) moved along similar paths from Lake Erie southwest over Redbank Creek at storm speeds approaching 100 km h^{-1} . Storm 4 (Fig. 18d) moved over the same path but at somewhat lower speed. Storms 1, 2, and 3 produced damaging winds and copious lightning but did not exhibit the mesocyclone signatures of supercell storms. The fourth storm element was a “borderline supercell” (Pearce et al. 1998) and produced a tornado in the Redbank Creek basin at 1330 UTC.

The Redbank Creek storms can be contrasted with the Orlando and Nebraska storms as a third setting in which supercell storms contribute to extreme flooding. The Orlando storm illustrates that an individual storm can produce extreme rainfall rates in small area and short time intervals. The Nebraska storms represent a

setting in which a series of supercell storms produces extreme flooding. The Redbank Creek storms represent a storm setting in which supercell storms combine with other storms to produce extreme floods.

An open question is how peak rainfall rates from supercell storms compare with rainfall rates from other forms of convective storms. For the Redbank Creek storm, a rain gauge at Brookville, Pennsylvania (see location in Fig. 19), was located in the path of all four storms. The storm total rainfall accumulation was 233 mm, of which 33 mm were recorded during a period of approximately 10 min (rainfall rate of 200 mm h^{-1}) from the periphery of the supercell storm. Rainfall accumulations to the southwest of the Brookville gauge likely were significantly larger because of a combination of higher rainfall rates and longer rainfall duration.

The storm total rainfall distribution (Fig. 19) reflects southeast motion of the storm elements. Tracks of the four storm elements cover the same area, producing a

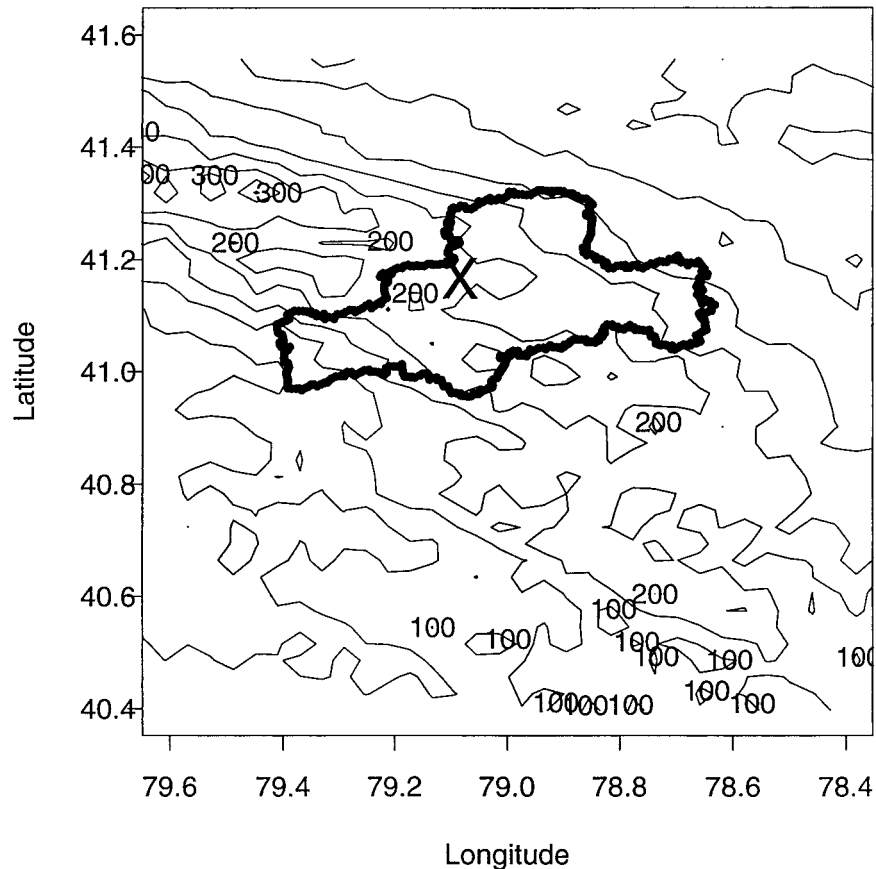


FIG. 19. Storm total rainfall (mm) field (0000–1600 UTC 19 Jul 1996) derived from volume-scan WSR-88D reflectivity observations using the WSR-88D $Z-R$ relationship ($Z = 300R^{1.4}$) and a 55-dBZ reflectivity threshold. Basin boundaries for Redbank Creek are shown. The location of the Brookville gauge is denoted by an "X."

narrow swath of heavy rainfall oriented from northwest to southeast. During the period of peak fractional coverage of heavy rainfall (Fig. 20) from 0800 to 0915 UTC, heavy rainfall covered an area of more than 500 km². Fractional coverage of heavy rainfall from the supercell storm produced an area of more than 400 km² with heavy rainfall in the lower portion of the Redbank Creek watershed. The contribution of the supercell storm was to produce the rapid increase of the Redbank Creek hydrograph to its peak discharge. Extreme rainfall from the supercell storm occurred in the lower portion of the basin (Fig. 20) and fell on terrain that had been moistened by the previous storms of the sequence.

6. Summary and observations

There are 10 principal observations from our work.

- 1) The Dallas Supercell resulted in 16 flash-flood deaths in the Dallas metropolitan area and more than \$1 billion in property damages over the Dallas–Fort Worth metroplex. Peak storm total rainfall for Dallas of 120 mm was not exceptional for Texas.
- 2) Rainfall rates from the Dallas Supercell were most exceptional at 15–60-min time intervals. Peak rainfall rates at 5- (231 mm h⁻¹), 15- (210 mm h⁻¹), and 60-min (115 mm h⁻¹) time intervals from the Dallas Supercell were 87%, 110%, and 115% of the 100-yr rainfall rates for the region. Peak rainfall rates for the Orlando Supercell were most extreme at 1–5-min timescales. The peak 1-min rainfall rate was 330 mm h⁻¹. The peak 5-min rainfall rate of 222 mm h⁻¹ is 85% of the 100-yr rainfall rate for east Florida.
- 3) Catastrophic flash flooding in Dallas resulted from three elements of storm motion: (a) motion of the supercell precipitation cascade centered at the inflow notch, (b) motion of the rear-flank downdraft of the supercell, and (c) motion of the trailing squall line. Fundamental differences in rainfall distribution and resulting flood response between the Orlando and Dallas storms are linked to the contrasting storm motion. The uniformly rapid storm motion of the Orlando storm resulted in concentration of heavy rainfall on smaller timescales and space scales than for the Dallas storm.

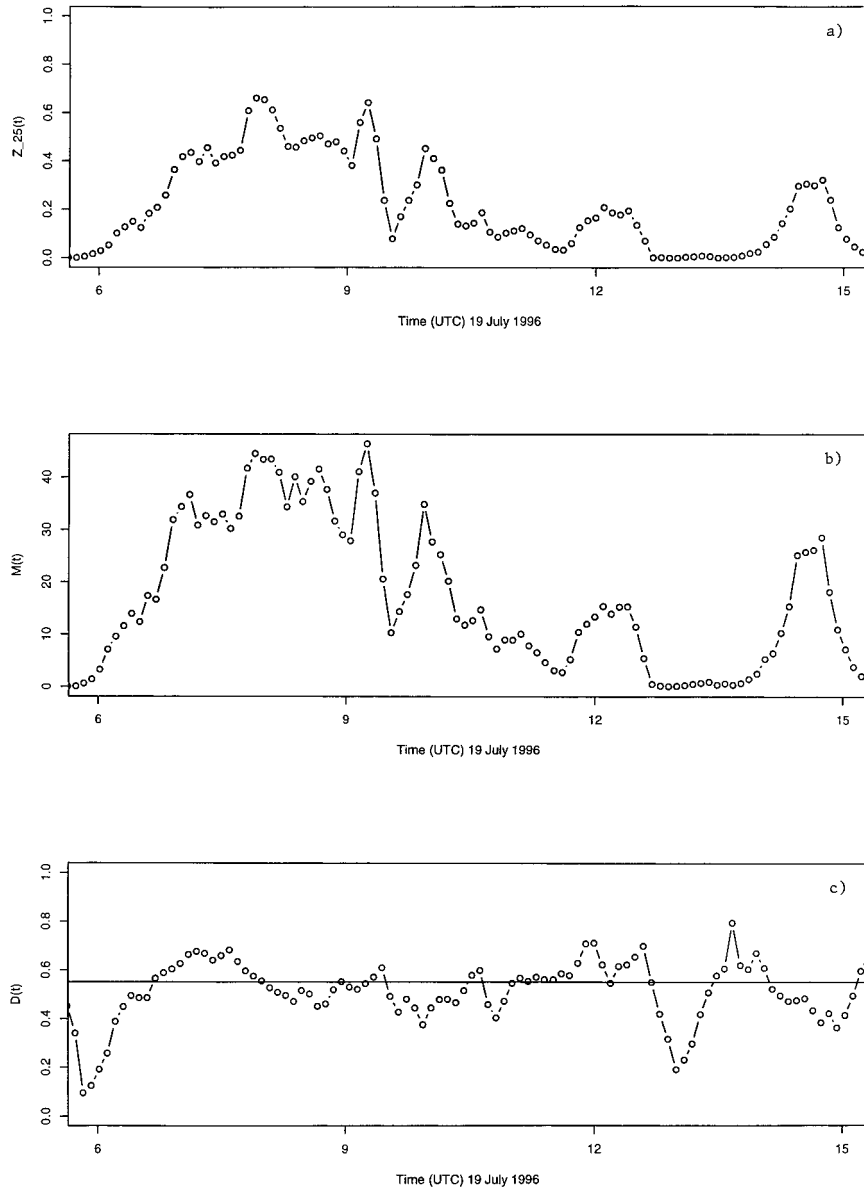


FIG. 20. Time series of (a) fractional coverage of heavy rainfall [$Z_{25}(t)$; fraction of basin area with rain rate $>25 \text{ mm h}^{-1}$], (b) basin-averaged rainfall (mm h^{-1}), and (c) normalized distance function (see text) for Redbank Creek.

- 4) Spatial variations of rainfall rate were associated with supercell structure for both the Dallas and the Orlando Supercells. For the Dallas Supercell, combined analyses of rain gauge and radar observations showed that distinct maxima in rainfall were organized around the precipitation cascade and rear-flank downdraft.
- 5) Systems of multiple supercell storms can produce extreme flooding at basin scales significantly larger than 100 km^2 . The 20–21 June 1996 flood episode in eastern Nebraska was produced by a series of tornadic, supercell storms. Four storms tracked over the 528-km^2 Pebble Creek catchment during a period of less than 4 h.
- 6) The flood occurrence behavior of eastern Nebraska has a sharp seasonal maximum around 20 June, which coincides closely with the maximum in tornado occurrence for the region. For Maple Creek, 6 of the largest 14 flood peaks can be linked to tornadic storms.
- 7) The western margin of the Appalachian region has experienced some of the largest measured rainfall accumulations in the world at short time intervals (less than 6 h). All are associated with severe thun-

- derstorms, and the maximum in heavy rainfall for the region is tightly concentrated around 19 July. The 18–19 July 1996 flooding in western Pennsylvania was produced by a series of severe thunderstorms that tracked rapidly from northwest to southeast. The final storm element that passed through Redbank Creek was a tornadic supercell storm.
- 8) For the Orlando and Dallas Supercells, extreme rainfall rates were produced during the dissipating phase of the storm. For the Nebraska storm, extreme rainfall and flooding in Pebble Creek resulted from a succession of supercell storms that produced seven tornadoes in and adjacent to Pebble Creek. Similar, for the Redbank Creek flood episode, flood-producing rainfall and a tornado were produced at the same time.
 - 9) Fundamental rainfall measurement problems exist for supercell storms. Measurements from conventional radar are very useful but are limited in estimating extreme rainfall rates because of problems associated with hail contamination and anomalous raindrop size distributions (relative to those assumed in deriving standard $Z-R$ relationships). Conventional rain gauge networks do not sample supercell rainfall at relevant space scales and timescales. Radar polarimetric measurements provide a promising avenue for overcoming the hail problem and problems associated with anomalous raindrop spectra (Zrnić and Ryzhkov 1999).
 - 10) Supercell thunderstorms play a significant role in determining the occurrence pattern of extreme rainfall rates at short timescales and small spatial scales for much of the United States east of the Rocky Mountains. These storms are of particular significance for urban hydrological behavior because of the fundamental role of extreme 1–30-min rain rates for design and water management problems in urban regions. As noted above, it is difficult to assess the climatological role of supercell storms from radar and conventional rain gauge networks. New observing systems and novel analysis procedures are needed to characterize the contributions of these storms to the occurrence of extreme rainfall precisely.
- Acknowledgments.* This research was funded in part by the U.S. Army Research Office (Grant DAAD19-99-1-0163), the National Science Foundation (Grant EAR-99-09696), NASA (Grant NAG5-7544), and NWS. This support is gratefully acknowledged. The comments and suggestions of an anonymous reviewer were most helpful in revising the manuscript.
- REFERENCES
- Baeck, M. L., and J. A. Smith, 1998: Estimation of heavy rainfall by the WSR-88D. *Wea. Forecasting*, **13**, 416–436.
- Band, L. F., E. Schroeder, and B. Hampton, 1982: Techniques for estimating magnitude and frequency of floods in the Dallas metropolitan area. Water Resources Investigation Rep. 82-18, U.S. Geological Survey, 55 pp.
- Bosart, L. F., and F. Sanders, 1981: The Johnstown flood of July 1977: A long-lived convective system. *J. Atmos. Sci.*, **38**, 1616–1642.
- Costa, J. E., 1987: Hydraulics and basin morphometry of the largest flash floods in the conterminous United States. *J. Hydrol.*, **93**, 313–338.
- Cotton, W. R., and R. A. Anthes, 1989: *Storm and Cloud Dynamics*. Academic Press, 883 pp.
- Dalrymple, T., 1937: Major Texas floods of 1935. U.S. Geological Survey Water-Supply Paper 796-G, 287 pp.
- Dixon, M., and G. Wiener, 1993: TITAN: Thunderstorm Identification, Tracking, Analysis, and Nowcasting—a radar-based methodology. *J. Atmos. Oceanic Technol.*, **10**, 785–797.
- Doswell, C. A., III, 1998: Seeing supercells as heavy rain producers. Preprints, *14th Conf. on Hydrology*, Dallas, TX, Amer. Meteor. Soc., 73–79.
- , and D. W. Burgess, 1993: Tornadoes and tornadic storms: A review of conceptual models. *The Tornado: Its Structure, Dynamics, Hazards and Prediction, Geophys. Monogr.*, No. 79, Amer. Geophys. Union, 161–172.
- , H. E. Brooks, and R. A. Maddox, 1996: Flash flood forecasting: An ingredients-based methodology. *Wea. Forecasting*, **11**, 560–581.
- Eisenlohr, W. S., Jr., 1952: Floods of July 18, 1942 in north-central Pennsylvania. U.S. Geological Survey Water-Supply Paper 1134-B, 100 pp.
- Erskine, H. M., 1951: Flood of August 4–5, 1943, in central West Virginia. U.S. Geological Survey Water-Supply Paper 1134-A, 47 pp.
- Finley, J. P., 1889: Local storms. *Mon. Wea. Rev.*, **17**, 184.
- Foufoula-Georgiou, E., and L. L. Wilson, 1990: In search of regularities in extreme rainstorms. *J. Geophys. Res.*, **95**, 2061–2072.
- Frederick, R. H., V. A. Myers, and E. P. Auciello, 1977: Five- to 60-minute precipitation frequency for the eastern and central United States. NOAA Tech. Memo. NWS Hydro-35, 35 pp.
- Groisman, P. Y., and D. R. Legates, 1994: The accuracy of United States precipitation data. *Bull. Amer. Meteor. Soc.*, **75**, 215–227.
- Gupta, V. K., O. Mesa, and D. R. Dawdy, 1994: Multiscaling theory of flood peaks: Regional quantile analysis. *Water Resour. Res.*, **30**, 3405–3421.
- Jennings, A. H., 1950: World's greatest observed point rainfalls. *Mon. Wea. Rev.*, **78**, 4–5.
- Lemon, L. R., and C. A. Doswell III, 1979: Severe thunderstorm evolution and mesocyclone structure as related to tornadogenesis. *Mon. Wea. Rev.*, **107**, 1184–1197.
- Miller, A. J., 1990: Flood hydrology and geomorphic effectiveness in the central Appalachians. *Earth Surf. Proc.*, **15**, 119–134.
- Moller, A. R., C. A. Doswell III, and R. Przyblinski, 1990: High-precipitation supercells: A conceptual model and documentation. Preprints, *16th Conf. Severe Local Storms*, Kananaskis Park, AB, Canada, Amer. Meteor. Soc., 52–57.
- , —, M. P. Foster, and G. R. Woodall, 1994: The operational recognition of supercell thunderstorm environments and storm structures. *Wea. Forecasting*, **9**, 327–347.
- NOAA, 1991: National disaster survey report: 20 June 1990 Shadyside, Ohio, flash flood. National Weather Service, Silver Spring, MD, 43 pp.
- , 1995: National disaster survey report: The Fort Worth–Dallas hailstorm and flash flood of May 5, 1995. National Weather Service, Silver Spring, MD, 39 pp.
- NRC, 1994: *Estimating Bounds on Extreme Precipitation Events*. National Academy Press, 30 pp.
- Pearce, M. L., G. S. Forbes, and E. Ostuno, 1998: Storm-scale aspects of non-classic, borderline supercell thunderstorms over Pennsylvania. Preprints, *16th Conf. on Weather Analysis and Forecasting*, Phoenix, AZ, Amer. Meteor. Soc., 109–111.
- Przyblinski, R. W., 1995: The bow echo: Observations, numerical simulations and severe weather detection methods. *Wea. Forecasting*, **10**, 203–218.
- Riedel, J. T., and L. C. Schreiner, 1980: Comparison of generalized estimates of probable maximum precipitation with greatest ob-

- served rainfalls. NOAA Tech. Rep. NWS 25, Office of Hydrology, Silver Spring, MD, 66 pp.
- Showalter, A. K., 1941: Meteorology of the storm. Flood of August 1935 in the Muskingum River basin, Ohio. C. V. Youngquist and W. B. Langbein, Eds., U.S. Geological Survey Water-Supply Paper 869, 29–31.
- Smith, J. A., 1992: The representation of basin scale in flood peak distributions. *Water Resour. Res.*, **28**, 2993–2999.
- , M. L. Baeck, J. E. Morrison, and P. Sturdevant-Rees, 2000: Catastrophic rainfall and flooding in Texas. *J. Hydrometeor.*, **1**, 5–25.
- Weisman, M. L., and J. B. Klemp, 1986: Characteristics of isolated convective storms. *Mesoscale Meteorology and Forecasting*, P. S. Ray, Ed., Amer. Meteor. Soc., 331–358.
- WMO, 1986: Manual for estimation of probable maximum precipitation. 2d ed. WMO No. 332, 250 pp.
- Woods, R., and M. Sivapalan, 1999: A synthesis of space–time variability in storm response: Rainfall, runoff generation and routing. *Water Resour. Res.*, **35**, 2469–2485.
- Zrnić, D. S., and A. V. Ryzhkov, 1999: Polarimetry for weather surveillance radar. *Bull. Amer. Meteor. Soc.*, **80**, 389–406.